

Laser cooling and trapping of Yb from a thermal source

U.D. Rapol, A. Krishna, A. Wasan, and V. Natarajan^a

Department of Physics, Indian Institute of Science, Bangalore 560 012, India

Received 27 February 2003 / Received in final form 15 February 2004

Published online 23 March 2004 – © EDP Sciences, Società Italiana di Fisica, Springer-Verlag 2004

Abstract. We have successfully loaded a magneto-optic trap for Yb atoms from a thermal source without the use of a Zeeman slower. The source is placed close to the trapping region so that it provides a large flux of atoms that can be cooled and captured. The atoms are cooled on the $^1S_0 \leftrightarrow ^1P_1$ transition at 398.9 nm. We have loaded all seven stable isotopes of Yb into the trap including the rarest isotope, ^{168}Yb . For the most abundant isotope (^{174}Yb), we load more than 10^8 atoms into the trap within 1 s. We have characterized the source by studying the loading rate and the loss rate for different isotopes and at different trapping powers. We extract values for the loss rate due to collisions and due to branching into low-lying metastable levels. At the highest trap densities, we find evidence of additional loss due to intra-trap collisions.

PACS. 32.80.Pj Optical cooling of atoms; trapping – 42.50.Vk Mechanical effects of light on atoms, molecules, electrons, and ions

1 Introduction

Laser-cooled atoms open exciting new possibilities for several experiments including those in precision spectroscopy. Yb is a particularly good choice for such studies because of several reasons. Yb has been proposed for experiments in quantum optics [1,2] due to the existence of two nearly-closed low-lying excited states with widely differing lifetimes. Laser-cooled Yb has been proposed for optical frequency standards applications [3]. Yb has been shown to be a useful candidate for the test of electroweak interactions because there is an enhanced parity-violation effect in the $^1S_0 \leftrightarrow ^3D_1$ transition [4]. Laser-cooled Yb extends the possibilities in measuring the strength of parity-violating interactions with unprecedented accuracy due to the availability of dense samples where one can apply large electric fields and homogeneous magnetic fields. Furthermore, Yb has a wide range of stable isotopes, both fermionic and bosonic, allowing one to explore the possibility of studying the properties of fermion-boson mixtures [5–7], especially in the quantum degenerate regime.

The starting point of most laser-cooling experiments is the magneto-optic trap (MOT) [8]. The source of atoms for the MOT is usually an oven inside the vacuum chamber containing a small amount of pure metal which is heated to release a beam of atoms. For atoms with high melting point such as Na, the hot atoms emanating from the oven are first slowed by a counter-propagating laser beam (Zeeman slower or chirp slower). Yb has a melting point of 819 °C and previous experiments have used a Zeeman slower for loading the MOT [9,11]. The main advantage of

using a slower is that the atomic beam can be turned off quickly by the use of shutters. However, we have earlier shown that a MOT for Rb atoms can be loaded efficiently from a thermal getter source operating at temperatures near 300 °C without the use of a slower [12]. Since Yb has considerable vapor pressure over the solid at 300 °C, we have been exploring the possibility of loading a Yb MOT directly from a thermal source.

In this paper, we show that this is indeed possible by successfully loading all the seven stable isotopes of Yb into the MOT from a thermal source. For the most abundant isotope (^{174}Yb), we load more than 10^8 atoms with a time constant of 300 ms. Most significantly, we can trap the rarest isotope (^{168}Yb) which has a natural abundance of only 0.13%. There are two factors that make such efficient trapping possible. The first is that the oven is placed close to the trapping region so that it provides a large flux of atoms that can be captured by the MOT. The second factor is that the excited state lifetime of the cooling transition is only 5.68 ns and the photon scattering rate is very high. Atoms are slowed over a short distance and small laser beams of 10 mm diameter are enough to cool and capture atoms from the background vapor. While this short lifetime implies a higher Doppler cooling limit, Yb has a second cooling transition with an extremely low Doppler limit, which can be used for further cooling the atoms. Indeed, this feature of having two widely-differing cooling transitions exists for other atoms such as Sr and Ca, and the techniques presented here have similar advantages in those species. For example, atoms could be first captured from a thermal vapor in a relatively low-vacuum region, and then transferred through a

^a e-mail: vasant@physics.iisc.ernet.in

differentially-pumped line to another MOT operating on the narrow cooling transition where the vacuum (and trap lifetime) is orders of magnitude better. The second MOT will provide ultra-cold atoms for further experiments in precision spectroscopy or optical dipole-force trapping.

There have been previous experiments where a Yb MOT has been loaded from an effusive source [7,11]. In reference [11], with the use of a Zeeman slower, about 10^7 atoms of ^{174}Yb were loaded into the MOT. However, without the Zeeman slower, the trap population was 20 times smaller, and ^{168}Yb could not be trapped. More recently, in reference [7], a bichromatic MOT for two-isotope trapping was loaded from a thermal source. However, only 3×10^5 atoms of ^{174}Yb were trapped in the two-isotope MOT with 15 mW of trapping power, and 10^7 atoms were trapped in the single-isotope MOT with 80 mW of trapping power. All these trap populations are significantly smaller than the values reported in this work. We have also studied the trap loss mechanisms in detail and have been able to separate the loss rate due to collisions and the loss rate due to decay into metastable states. At large trap densities, we begin to see the effect of non-linear losses due to intra-trap collisions.

2 Experimental details

Yb has two possible cooling transitions, as seen from the energy level diagram in Figure 1. The $^1\text{S}_0 \leftrightarrow ^3\text{P}_1$ intercombination line at 555.8 nm forms a pure two-level system in Yb due to the absence of ground-state hyperfine structure. The transition has a long lifetime of 874 ns corresponding to a natural linewidth of $\Gamma = 2\pi \times 182$ kHz, and therefore the photon cycling rate is very slow. However, the Doppler cooling limit is $4 \mu\text{K}$, a very desirable temperature for high-precision measurements. The other cooling transition is the $^1\text{S}_0 \leftrightarrow ^1\text{P}_1$ transition at 398.9 nm. This has a short lifetime of 5.68 ns corresponding to a linewidth of $\Gamma = 2\pi \times 28$ MHz, and allows photons to be cycled quickly. However, it has the disadvantage of giving a high Doppler cooling limit of $670 \mu\text{K}$, and is not a completely closed transition since the excited state can branch into the low-lying ^3P levels through the intermediate ^3D levels. Despite these disadvantages, we have used the 398.9 nm transition for our experiments primarily because the high photon scattering rate allows atoms to be cooled over a short distance.

The laser light for the 398.9 nm transition is produced in a two-step process. First, the output of a tunable Ti-sapphire laser (Coherent 899-21) is set to half the desired frequency near 798 nm. Then its output is fed into an external-cavity frequency-doubling unit (Laser Analytical Systems, LAS100) which uses a nonlinear crystal of lithium triborate to produce the desired 398.9 nm light. The Ti-sapphire laser is actively stabilized using an ovenized, Fabry-Perot reference cavity and its instantaneous linewidth is less than 1 MHz. We have also measured that the laser's long-term drift is only a few MHz per hour, so that it is unnecessary to lock the laser to an external reference during the trapping experiment. We find that it

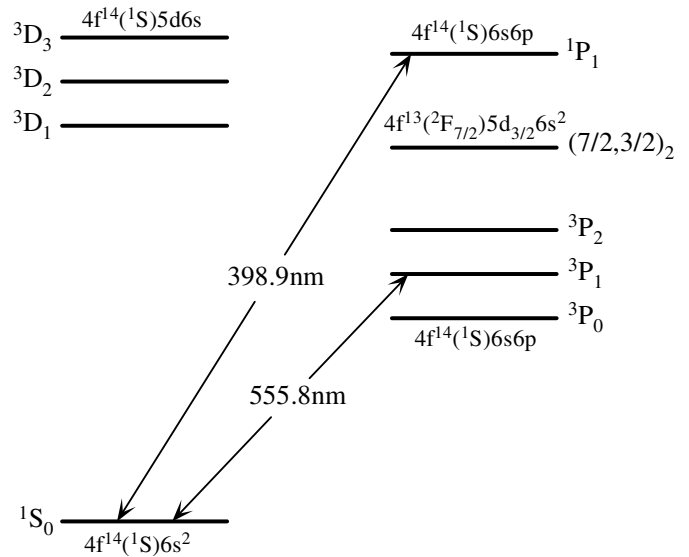


Fig. 1. Yb energy levels. The figure shows the relevant low-lying energy levels in Yb. Even-parity states are on the left and odd-parity states on the right. The two possible cooling transitions at 398.9 nm and 555.8 nm are shown.

is sufficient to set the frequency at the desired point and leave it there for the duration of the experiment. The frequency is set using a home-built wavemeter [13] that uses a scanning Michelson interferometer and a Rb-stabilized reference laser. The wavemeter has an absolute accuracy of a few MHz which is more than sufficient for finding the Yb lines. Once the trap is working, the trap fluorescence signal is used to optimize the laser detuning, Δ .

The experiments are done inside a glass cell pumped by a 20 l/s ion pump and maintained at a pressure below 10^{-9} Torr. The source of Yb atoms is a quartz ampoule containing a small amount of elemental Yb. The ampoule is a 30 mm long tube of 5 mm diameter that is sealed at one end and constricted to 1 mm diameter at the other end. The constriction seems important both in ensuring a uniform flux in the trapping volume and in preventing the walls from getting coated with a film of Yb. Using a collimated thermal beam, as is the case when using a Zeeman slower, causes the opposite wall to get rapidly coated with a thick film of Yb. On the other hand, we find no such deposit even after 50 hours of operation of the source. The source is placed about 50 mm from the trap center. It is resistively heated to a temperature of 300–400 °C to release Yb. At 400 °C, the vapor pressure of Yb is 6×10^{-5} Torr.

The MOT is formed from a standard configuration consisting of three sets of mutually orthogonal laser beams and a quadrupole magnetic field superposed at the intersection of the beams. The total laser power available near the MOT can be varied up to 120 mW. This is split into three circularly-polarized beams. The three beams have equal power and $1/e^2$ diameter of 10 mm. Since the saturation intensity I_0 for the transition is 58 mW/cm^2 , the peak intensity in each beam is $0.9I_0$ when the total laser power is 120 mW. The beams are retroreflected after passing

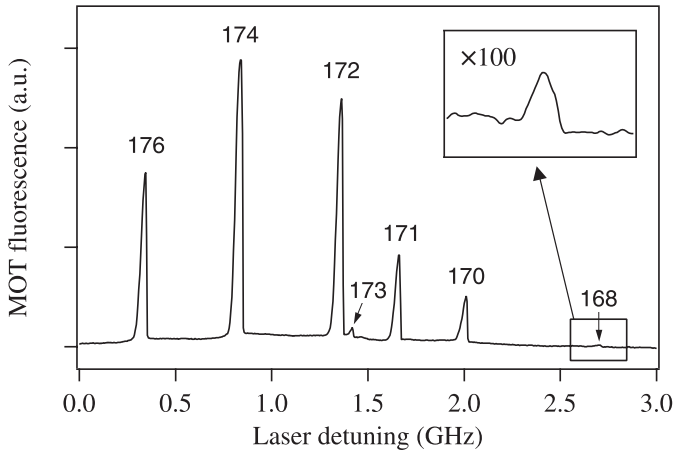


Fig. 2. MOT fluorescence vs. laser detuning. The fluorescence signal shows peaks as each isotope comes into resonance with the laser and is trapped in the MOT. Each peak is labeled by the corresponding isotope number. The inset shows a $100\times$ magnified view of the region where ^{168}Yb is trapped.

through the cell, and the intensity in the return beams is slightly smaller due to losses along the optical path. The quadrupole magnetic field is produced using a pair of coils (270 turns each) placed 40 mm apart. With 3 A of current through the coils, the field gradient at the center is 90 G/cm. The fluorescence from the trapped atoms is collected by a lens subtending a solid angle of 0.07 sr and imaged on to a calibrated photo-multiplier tube (PMT). The number of trapped atoms is estimated from the total power incident on the PMT after accounting for losses along the optical path [12]. There is an error of about 20% in estimating the number of atoms in this manner, but relative values between isotopes and other such trends are unaffected by this error.

3 Results and discussion

In the first set of experiments, we scanned the laser slowly across a frequency range of 3 GHz. The fluorescence signal detected by the PMT is shown in Figure 2. The signal shows peaks as each isotope comes into resonance and gets trapped in the MOT. The peak heights correspond roughly to the natural abundance of each isotope except for the odd isotopes which show anomalous behavior. This is because the odd isotopes have half-integer nuclear spin and consequently have hyperfine structure in the $^1\text{P}_1$ excited state. In these cases, optical pumping in the ground state causes additional loss from the trap [9]. The signal from the rarest isotope ^{168}Yb is also seen in the figure. As shown in the inset of Figure 2, the ^{168}Yb peak becomes clearer when the gain of the PMT is increased by a factor of 100.

In order to better characterize the source and find optimal values for the laser detuning, we have studied the trap population as a function of laser frequency. The laser was scanned slowly over a frequency range of 100 MHz below the resonance. The results for ^{174}Yb are shown in

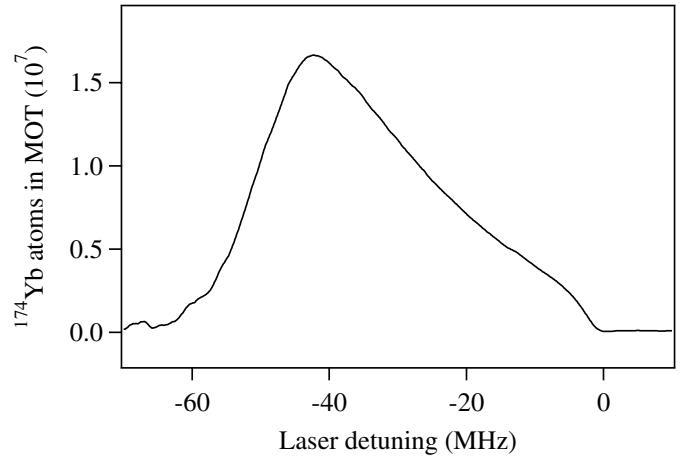


Fig. 3. Number of trapped atoms vs. detuning. The number of ^{174}Yb atoms in the MOT is shown as the detuning of the laser is varied slowly from -60 MHz (-2Γ) to 0. The magnetic field gradient at the trap center was 75 G/cm. The number of atoms shows a peak at -42 MHz or -1.5Γ . Other isotopes show identical behavior.

Figure 3. The number of trapped atoms shows a peak value of 1.7×10^7 at a detuning of -1.5Γ . This is similar to the behavior seen in the case of a Rb MOT loaded from a thermal source [12]. Note that the optimal value of detuning depends on the size of the trapping beams and the magnetic-field gradient, since both these parameters are important in determining the distance over which atoms are slowed and captured. The data in Figure 3 were taken with a magnetic field gradient of 75 G/cm. All the other isotopes show similar dependence on detuning.

The loading of the MOT from a thermal source follows a rate equation [12, 14]

$$\frac{dN}{dt} = R - \frac{N}{\tau} - \beta N^2, \quad (1)$$

where N is the number of atoms in the trap, R is the rate at which atoms are captured from the source, $1/\tau$ is the linear loss rate from the trap, and β gives the nonlinear losses due to intra-trap collisions. In the case of Yb, there are two factors that contribute to the linear loss rate. The primary mechanism is collisional loss, both due to collisions with background atoms and collisions with hot, untrapped Yb atoms. In addition, as mentioned before, the $^1\text{P}_1$ excited state of the cooling transition can branch into the low-lying ^3P levels. Of these, the $^3\text{P}_0$ and $^3\text{P}_2$ levels are metastable levels; atoms shelved into these levels no longer participate in the cooling cycle and are rapidly lost from the trap [11].

We have characterized the thermal source by studying in turn each of the three terms in equation (1). We first consider the loading rate R by studying the loading characteristics of the MOT for the different isotopes. If the nonlinear loss term is neglected, the solution to equation (1) is an exponential growth in the number of trapped atoms: $N = N_s[1 - \exp(-t/\tau)]$, where N_s is the steady state population and is given by $R\tau$. The loading characteristics of the most abundant isotope ^{174}Yb

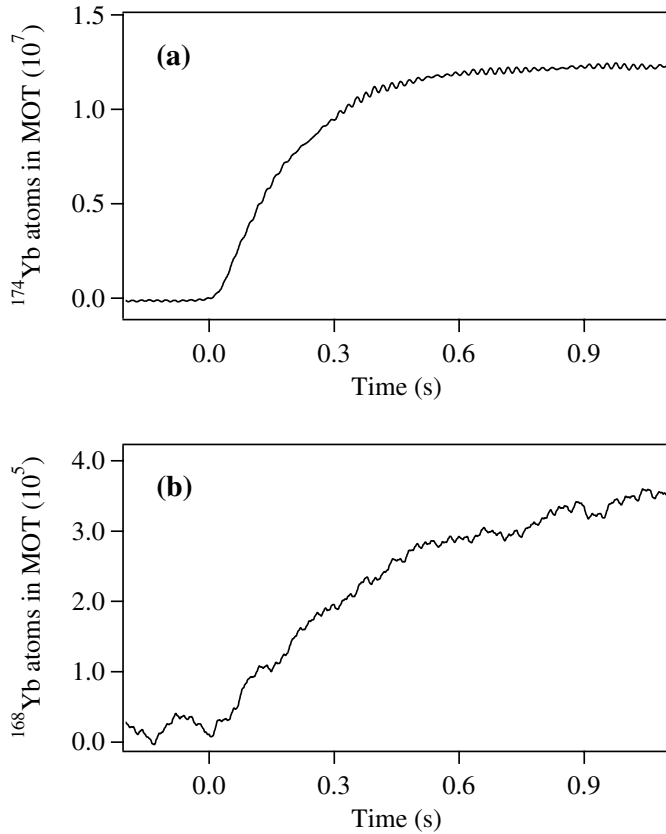


Fig. 4. Loading of the MOT. The build up of the number of atoms in the MOT is shown after the trapping beams are turned on at $t = 0$. In (a), we have a MOT for ^{174}Yb at a detuning of -1.2Γ and field gradient of 75 G/cm. In (b), we observe signal from a MOT for ^{168}Yb at a detuning of -1.2Γ and field gradient of 60 G/cm. Both curves show exponential growth in the number of atoms with time constants of 190 ms and 440 ms, respectively. Note that under steady state, the number of trapped ^{168}Yb atoms is about 40 times smaller.

and the least abundant isotope ^{168}Yb are shown in Figure 4. Both curves follow the exponential behavior predicted from equation (1) and there is no significant deviation even when the trap population is high. We conclude that under these conditions, intra-trap collisional loss is insignificant. From Figure 4, we see that for ^{174}Yb the time constant is 190 ms and the steady state population is 1.3×10^7 . For ^{168}Yb , the time constant is 440 ms while the steady state population is about 40 times smaller. It is also interesting that the optimal value of magnetic-field gradient for trapping ^{174}Yb and ^{168}Yb are different, with values of 75 G/cm and 60 G/cm, respectively. The fine oscillations present in the signal (especially in Fig. 4a) are due to trap instabilities that are well known in MOTs of other atoms. They are suppressed by careful adjustment of the beam alignment and polarizations.

The characteristics of the source become more apparent by studying the values of τ and N_s for the different isotopes under identical conditions. The measured values are listed in Table 1. The data were taken at a detuning of -1.2Γ and field gradient of 75 G/cm. The value

Table 1. Listed are the loading time constant τ and steady state population N_s in the MOT for the various isotopes. The data for each isotope were taken at a detuning of -1.2Γ and field gradient of 75 G/cm. The errors in τ are statistical 1σ deviations. For N_s , there is a calibration error of about 20% due to errors in converting the detected fluorescence signal to the number of atoms. However, the error is the same for all isotopes and does not affect relative values.

Isotope	Nat. abund.	N_s	τ (ms)
176	12.7%	8.0×10^6	300(30)
174	31.8%	1.3×10^7	190(10)
172	21.9%	1.1×10^7	260(20)
173	16.1%	1.7×10^6	440(25)
171	14.3%	3.4×10^6	165(10)
170	3.05%	3.0×10^6	450(30)

Table 2. Listed are the loading rate R and steady state population N_s for the various isotopes from Table 1, normalized to the values for ^{174}Yb . For the even isotopes, the loading rate scales as the isotopic abundance, as expected for a non-enriched thermal source. The odd isotopes show different behavior due to excited-state hyperfine structure.

Isotope	Rel. abund.	R/R^{174}	N_s/N_s^{174}
176	0.40	0.39(4)	0.62
174	1.00	1.00	1.00
172	0.69	0.61(5)	0.85
173	0.51	0.055(4)	0.13
171	0.45	0.30(2)	0.26
170	0.096	0.096(8)	0.23

of τ for the different isotopes lies in the range of 160–450 ms, while N_s varies from 3×10^6 to 1.3×10^7 . The general trend is that τ decreases and N_s increases with the natural abundance of the isotope, except for the odd isotopes which, as mentioned before, show anomalous behavior due to excited-state hyperfine structure. The trends become clearer when we consider the values for the loading rate and N_s for each isotope normalized to the corresponding value for ^{174}Yb , as listed in Table 2. For the even isotopes, the normalized loading rate is equal to the relative abundance, exactly as expected from a non-enriched source. Interestingly, the value of N_s/N_s^{174} is larger than the relative abundance.

The above experiments were done in a Pyrex cell. To improve the optical quality of the trapping beams, we have recently changed to a quartz cell with high-quality windows. We have also optimized the location of the source with respect to the trapping region and improved the base pressure in the vacuum chamber. This has given us an order of magnitude improvement in the trap population. It has also allowed us to study the loss mechanisms more precisely. As mentioned earlier, the linear loss rate in equation (1) consists of two parts: one due to background collisions, and the other due to branching into metastable

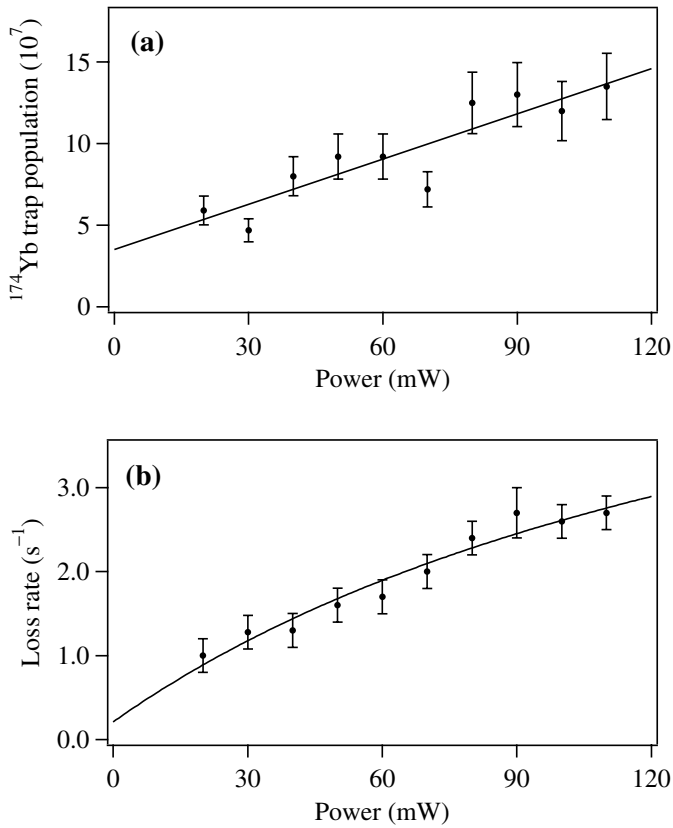


Fig. 5. Power dependence of the MOT. In (a), we show that the number of trapped ^{174}Yb atoms increases linearly with trapping power. In (b), we study the loss rate as a function of power. The solid line is a fit to equation (2) in the text and allows us to separate the loss rates due to collisions and branching into metastable levels.

levels. A simple model for this yields:

$$\frac{1}{\tau} = \alpha_b + \alpha_{2,0}f, \quad (2)$$

where α_b is the loss rate due to background collisions, $\alpha_{2,0}$ is the loss rate for excited-state atoms due to branching into the $^3\text{P}_2$ and $^3\text{P}_0$ levels, and f is the fraction of trapped atoms in the excited state. The excited-state fraction is given by:

$$f = \frac{1}{2} \frac{I/I_0}{1 + I/I_0 + (2\Delta/\Gamma)^2}, \quad (3)$$

where I is the total trapping-laser intensity. The loss rate due to the two effects can thus be separated by studying the trap characteristics at different trapping powers since this would change the excited-state fraction.

The results of such a study on ^{174}Yb are shown in Figure 5. In Figure 5a, we first show the increase in the trap population as the trapping power increases from 20 mW to 120 mW. This is not surprising since an increase in the trapping power increases the loading rate R . In Figure 5b,

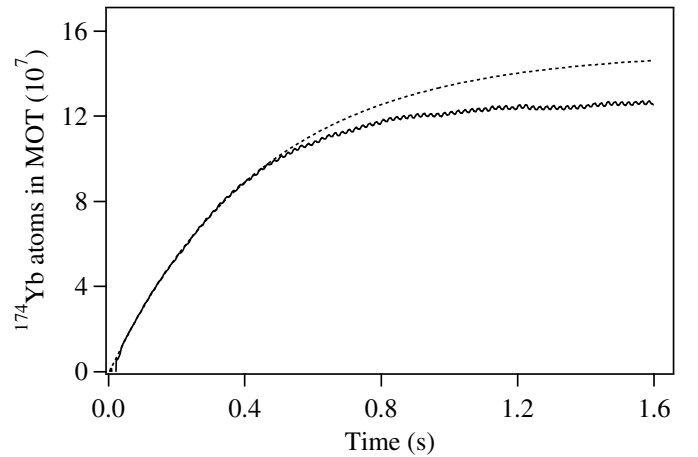


Fig. 6. Nonlinear losses. The number of ^{174}Yb atoms in the trap (solid line) increases exponentially at first, but saturates at a lower value due to the N^2 loss term in equation (1). The dotted line is the extrapolated exponential curve.

we show the loss rate as a function of trapping power. The solid line is a fit to equation (2). The intensity factor I/I_0 in equation (3) is modeled as kP , where P is the trapping power, and the proportionality constant k takes care of geometric factors such as overlap of the MOT beams, intensity profile across the beams, and variations in intensity due to losses in the retro-reflected beams. The constant k is left as an additional fit parameter to the data in Figure 5b. This is important because trying to calculate k from the experimental parameters leads to errors as large as 50% [11]. The fit yields values of $\alpha_b = 0.25(15)\text{ s}^{-1}$ and $\alpha_{2,0} = 13(3)\text{ s}^{-1}$. The value of α_b is comparable to the value of 0.2 s^{-1} for a Rb MOT loaded from a thermal source where the only loss mechanism is loss due to background collisions [12]. The value of $\alpha_{2,0}$ is consistent with the experimental value of $24(13)\text{ s}^{-1}$ and a theoretical estimate of $6(4)\text{ s}^{-1}$ quoted in reference [11]. We have also studied the effect of the proportionality constant k mentioned above by deliberately misaligning the trapping beams. This changes the total laser intensity for the trapped atoms at a given power, and therefore the value of k . We find that the value of $\alpha_{2,0}$ remains unaffected, giving us further confidence in the measured value.

Finally, we turn to the nonlinear loss term in equation (1) that arises due to intra-trap collisions. As expected, these losses are significant only at the highest trap densities which we have achieved in the quartz-cell trap. This is seen in Figure 6 where we plot the loading characteristics for ^{174}Yb in the improved trap. Initially, the number of trapped atoms grows exponentially. But as the trap population builds up, the growth curve deviates from the exponential and saturates at a lower value than what is expected by extrapolating the exponential. From the actual steady-state population and the loading time constant, we calculate $\beta = 1.7(4) \times 10^{-9}\text{ s}^{-1}$. This value is of the same order of magnitude as values obtained in a Rb MOT [10].

4 Conclusions

We have successfully loaded a MOT for Yb atoms from a thermal source without the necessity of a Zeeman slower. The source is placed close to the trapping region so that it provides a large flux of atoms that can be captured by the MOT. We have loaded all seven stable isotopes of Yb. For the most abundant isotope (^{174}Yb), we load about 10^8 atoms into the trap within 1 s. We have studied the trap population as a function of laser detuning and find that the population is maximized near a detuning of -1.5Γ . We have characterized the source by studying the loading of the MOT for different isotopes. We have also studied the loss rate as a function of trapping power. This allows us to separate the loss rate due to collisions from the loss rate due to branching into the low-lying metastable $^3\text{P}_0$ and $^3\text{P}_2$ levels. Under our conditions, the loss rate due to branching into these levels is much larger and the trap population is limited by this loss. In future, we plan to clear out these levels using diode lasers at 649 nm (exciting the $^3\text{P}_0 \rightarrow ^3\text{S}_1$ transition) and at 770 nm (exciting the $^3\text{P}_2 \rightarrow ^3\text{S}_1$ transition). With these improvements, we expect to increase the trap population and the lifetime by a factor of 3 to 5. The increased number and lifetime will be important for many of the proposed experiments using laser-cooled Yb.

We thank V. Anandan for fabricating the Pyrex cell. This work was supported by a research grant from the Department of Science and Technology, Government of India. One of us (A.W.) acknowledges financial support from CSIR, India.

References

1. D.J. Heinzen, J.J. Childs, J.E. Thomas, M.S. Feld, *Phys. Rev. Lett.* **58**, 1320 (1987)
2. A.M. Bacon, H.Z. Zhao, L.J. Wang, J.E. Thomas, *Phys. Rev. Lett.* **75**, 1296 (1995)
3. J.L. Hall, M. Zhu, P. Buch, *J. Opt. Soc. Am. B* **6**, 2194 (1989)
4. D. DeMille, *Phys. Rev. Lett.* **74**, 4165 (1995)
5. M.-O. Mewes, G. Ferrari, F. Schreck, A. Sinatra, C. Salomon, *Phys. Rev. A* **61**, 011403 (2000)
6. S.F. Crane, X. Zhao, W. Taylor, D.J. Vieira, *Phys. Rev. A* **62**, 011402 (2000)
7. T. Loftus, J.R. Bochinski, T.W. Mossberg, *Phys. Rev. A* **63**, 053401 (2001)
8. E.L. Raab, M. Prentiss, A. Cable, S. Chu, D. Pritchard, *Phys. Rev. Lett.* **59**, 2631 (1987)
9. K. Honda, Y. Takahashi, T. Kuwamoto, M. Fujimoto, K. Toyoda, K. Ishikawa, T. Yabuzaki, *Phys. Rev. A* **59**, R934 (1999)
10. D. Sesko, T. Walker, C. Monroe, A. Gallagher, C. Wieman, *Phys. Rev. Lett.* **63**, 961 (1989)
11. T. Loftus, J.R. Bochinski, R. Shivitz, T.W. Mossberg, *Phys. Rev. A* **61**, 051401 (2000)
12. U.D. Rapol, A. Wasan, V. Natarajan, *Phys. Rev. A* **64**, 023402 (2001)
13. A. Banerjee, U.D. Rapol, A. Wasan, V. Natarajan, *Appl. Phys. Lett.* **79**, 2139 (2001)
14. M.H. Anderson, W. Petrich, J.R. Ensher, E.A. Cornell, *Phys. Rev. A* **50**, R3597 (1994)